siRNA cell arrays for high-content screening microscopy

Holger Erfle, Jeremy C. Simpson, Philippe I.H. Bastiaens, and Rainer Pepperkok

European Molecular Biology Laboratory, Heidelberg, Germany

BioTechniques 37:454-462 (September 2004)

RNA interference (RNAi) is a recent advance that provides the possibility to reduce the expression of specific target genes in cultured mammalian cells with potential applications on a genome-wide scale. However, to achieve this, robust methodologies that allow automated and efficient delivery of small interfering RNAs (siRNAs) into living cultured cells and reliable quality control of siRNA function must be in place. Here we describe the production of cell arrays for reverse transfection of tissue culture cells with siRNA and plasmid DNA suitable for subsequent high-content screening microscopy applications. All the necessary transfection components are mixed prior to the robotic spotting on noncoated chambered coverglass tissue culture dishes, which are ideally suited for time-lapse microscopy applications in living cells. The addition of fibronectin to the spotting solution improves cell adherence. After cell seeding, no further cell culture manipulations, such as medium changes or the addition of 7serum, are needed. Adaptation of the cell density improves autofocus performance for high-quality data acquisition and cell recognition. The co-transfection of a nonspecific fluorescently labeled DNA oligomer with the specific siRNA helps to mark each successfully transfected cell and cell cluster. We demonstrate such an siRNA cell array in a microscope-based functional assay in living cells to determine the effect of various siRNA oligonucleotides against endogenous targets on cellular secretion.

INTRODUCTION

The completion of sequencing the genomes of a number of organisms now provides us with the opportunity to understand how these lists of genes give rise to cellular behavior governed through protein interaction networks. Within this framework, one goal of proteomics is to classify proteins according to their function. In order to do this, robust protocols need to be available that can be applied to large sets of molecules. Recently, Ziauddin and colleagues (1) have developed such a tool for the proteomics field, namely, a microarray of printed plasmid DNAs for reverse transfection of living cells. Such microarrays are prepared by first printing a coated glass slide with an array of plasmid DNAs. Transfection reagents are then overlaid and, finally, cells are plated onto these slides, resulting in clusters of cells that, with the help of the transfection reagent (reverse transfection), express the respective cDNAs at each location. While cDNA overexpression has certainly enhanced our understanding of gene function, the ability to selectively down-regulate genes is now proving even more powerful. In particular, RNA interference (RNAi) utilizing small interfering RNAs (siRNAs) is a recent advance that provides the possibility of reducing gene expression at the post-transcriptional level in cultured mammalian cells (2). This technique is one valuable step toward determining gene function and can be theoretically applied on a genome-wide scale (3).

Here we describe the development, testing, and application of a protocol for siRNA microarray production that allows spotting of the siRNAs and transfection reagents in only two steps. The procedure is sufficiently robust to be applied through automation on a large scale to the down-regulation of a variety of endogenous proteins. Furthermore, the quality of data obtained from this method is ideally suited for microscope-based functional assays designed to determine gene function in living cells.

MATERIALS AND METHODS

RNAi Oligonucleotides

Oligonucleotides (Qiagen, Valencia, CA, USA) used for RNAi were as follows. For human β-COP (GenBank® accession no. NM_016451), the target sequences were 161–181 nucleotides (5′-AACUUCCUGGACUUCUGAUGA-3′) and 1566–1586 nucleotides (5′-AACUCAGAGUGCCCUUAGCAG-3′) downstream from the ATG. For human GM130 (accession no. AF248953; BD Biosciences, San Jose, CA, USA), the target sequence was 543–563 nucleotides (5′-AAUUACGGAUCAGUUGGAAGA-3′), and for human Sec31 (accession no. AF139184), 529–549 nucleotides (5′-AACAGACAAGUUCAGCAUAUU-3′) downstream from the ATG. The target sequence of the control oligonucleotide was 5′-AAUUCUCCGAACGUGUCACGU-3′. As a control, a nonsilencing rhodamine-labeled siRNA (si control; si, small interfering) with the sequence 5′-UUCUCCGAACGUGUCACG-3′ was used.

In each case, pairs of complementary RNAs with 3′ dT overhangs were synthesized, annealed, and purified. Lyophilized oligonucleotide duplexes were resuspended in the supplied resuspension buffer (Qiagen) at 20 µM. The Cy™3-labeled DNA marker oligomer with the sequence 5′-TGACGTTCTATAGCGACGGCCAGT-3′ was obtained from BioSpring (Frankfurt, Germany). The labeling of oligomers with rhodamine or Cy3 was always at the 5′ end.

Preparation of Cell Arrays

The siRNA-gelatin transfection solution was prepared in 384-well plates (Nalge Nunc International, Rochester, NY, USA) as follows. Plasmid (500 ng) and/or 1 µL of siRNA solution (20 µM in RNA dilution buffer; Qiagen), and 7.5 µL EC buffer (Qiagen) containing 0.2 M sucrose were incubated for 10 min at room temperature, mixed with 4.5 µL Effectene® (Qiagen), and incubated for an additional 10 min at room temperature with 7.25 µL of 0.08% gelatin (Sigma-Aldrich, St. Louis, MO, USA) and 3.5×10^{-4}% fibronectin (Sigma-Aldrich).

For transfections with Oligofectamine™ (Invitrogen, La Jolla, CA, USA), 1 µL siRNA solution was added to 8.5 µL OptiMEM™ (Invitrogen) and incubated for 10 min. OptiMEM (1.6 µL) and 0.4 µL Oligofectamine were mixed and incubated for 10 min. These two separate solutions were subsequently mixed and incubated for another 10 min. Then, 8.5 µL of 0.2% gelatin and 30 µL of phosphate-buffered saline (PBS) were added.

In those experiments where a Cy3-labeled DNA oligonucleotide was used as transfection marker, 0.5 µL of a 40-µM marker solution was added together with the siRNA or DNA to be transfected. The solutions were arrayed onto single-well, chambered Lab-Tek™ coverglass tissue culture dishes (Nalge Nunc International) using a ChipWriter™ Compact Robot (Bio-Rad Laboratories, Hercules, CA, USA). Solid pins (Eurogentec, Seraing, Belgium) and SMP10™ quill pins (TeleChem International), resulting in a spot diameter of approximately 400 µm for all experiments, were used. The spot volume was approximately 4 nL. After printing, 1.25×10^5 HeLa, MCF7, COS7L, or HEK293 cells were plated on the Lab-Tek slide in a total volume of 2.5 mL culture medium [Dulbecco's modified Eagle's medium (DMEM) containing 10% heat-inactivated fetal calf serum (FCS), 2 mM glutamine, 100 U/mL penicillin, and 100 µg/mL streptomycin] and incubated for 44 h at 37°C and 5% CO_2.

Immunostaining of Cells and Transport Assay

For immunostaining, the cells were first fixed in -20°C methanol for 4 min, followed by 2 washes with PBS. The monoclonal antibody against β-COP (mAD; Reference 4) was applied for 10 min, followed by washing of the cells and incubation with anti-mouse Alexa488- (Molecular Probes, Eugene, OR, USA) or Cy5- (Amersham Biosciences, Piscataway, NJ, USA) conjugated secondary antibodies. Finally, Hoechst 33342 (1 µg/mL final concentration; Sigma-Aldrich) was added for 10 min to stain the cell nuclei. For the transport assay, cell arrays were prepared as above and then incubated for 26 h prior to infection with recombinant adenoviruses expressing cyan fluorescent protein (CFP)-tagged ts-O45-G for 1 h, followed by incubation at the restrictive temperature of 39.5°C for 16 h (5). Ts-O45-G was released from the endoplasmic reticulum (ER) at 32°C for 1 h in the presence of 100 µg/mL cycloheximide (Calbiochem, San Diego, CA, USA). The cells were fixed with 3.5% paraformaldehyde for 20 min prior to staining with antibodies against an extracellular epitope of the ts-O45-G protein (4). Secondary antibodies were prepared as described above.

Data Acquisition and Analysis

Images were acquired with Axio Vision™ 3.1 on an Axiovert™ 200M Microscope (Carl Zeiss, Rochester, NY, USA) equipped with a 20×/0.75 air Fluar® objective (Carl Zeiss) and an AxioCam HR™ CCD camera (Carl Zeiss). The filters used were standard filters (no. 34 for Hoechst, no. 6 for CFP, no. 44 for Alexa 488, no. 43 for Cy3 and rhodamine, and no. 26 for Cy5). Exposure times varied from 57 ms for Hoechst, 800 ms for CFP, 300 ms for GFP, and 500 ms for Cy3 and rhodamine to 6500 ms for Cy5 and were kept constant for all experiments.

The images were background-corrected by subtracting the average pixel value in a blank region of the image. Borders of the spot area could be estimated by Cy3 or rhodamine labeling of cells (Figure 1A). Transfection efficiencies were then determined by visual inspection and dividing the number of successfully transfected cells (indicated by their oligomer-specific Cy3 or rhodamine labeling (Figure 1) by the total number of cells in a spot area.

Quantification of single-cell fluorescence was performed with MetaMorph® (Universal Imaging, Downingtown, PA, USA). After background subtraction, a region around each cell of interest was defined manually (radius: 50 image pixels). In each region, the average intensity was measured, and the mean values with the standard deviation of the means for all regions were calculated. Intensities are expressed in arbitrary units.

The ts-O45-G transport efficiency was calculated by dividing for each cell the intensity obtained for the ts-O45-G at the cell surface (Cy5) by the intensity of the CFP-ts-O45-G within the cell. The average values obtained were then normalized to the si control (1.0) spotted on the same slide.

Western Blot Analysis

HeLa cells were cultured in 6-well plates prior to transfection with siRNA oligonucleotides against β-COP or GM130. For transfections with Oligofectamine, 10 µL siRNA solution were added to 170 µL OptiMEM and incubated for 10 min. Sixteen microliters of OptiMEM and 4 µL Oligofectamine were mixed and incubated for 10 min. These two separate solutions were subsequently mixed and incubated for another 20 min. The cells were washed once with serum-free medium and then overlaid with 800 µL of the same medium. The transfection mixture was added drop-wise to the cells, and then incubated for 4 h. Finally, the cells were overlaid with 500 µL of medium containing 30% serum (10% final concentration). After 44 h, the cells were lysed in radioimmunoprecipitation (RIPA) buffer [50 mM Tris, pH 7.2, 150 mM NaCl, 1% Triton® X-100, 1% sodium deoxycholate, 0.1% sodium dodecyl sulfate (SDS)], and the total protein concentrations were determined. Twelve micrograms of each extract were subjected to sodium dodecyl sulfate polyacrylamide gel electrophoresis (SDS-PAGE) on 10% gels followed by transfer to polyvinylidene difluoride (PVDF) membranes. Membranes were probed with antibodies against β-COP, GM130, or α-tubulin (Neomarkers, Fremont, CA, USA), followed by appropriate secondary antibodies and electrochemiluminescence (ECL) detection.

RESULTS AND DISCUSSION

In order to be able to apply reverse transfection to experiments in living cells, we decided to use chambered coverglass tissue culture dishes for spotting the cDNA and siRNA molecules. These have the advantage that they easily permit the cellular medium to be changed, facilitate automation of

immunostaining protocols and, most importantly, allow high-resolution functional assays in living cells on any inverted microscope.

For array production, we developed a two-step protocol in which, in the first step, the transfection reagent used is directly included with a gelatin/siRNA (DNA)/fibronectin mixture for the spotting on uncoated chambered coverglass tissue culture dishes.

The optimal range of fibronectin concentration was determined to be between 3.5×10^{-4}% and 5.25×10^{-4}%. In this range, the transfection efficiency increased 1.5-fold, and cell adherence 2-fold per spot, compared to the same solution without fibronectin. We used 3.5×10^{-4}% fibronectin for further experiments.

For a spot diameter of 400 µm and a spot-to-spot distance of 1125 µm, one can apply 384 samples per Lab-Tek chamber. Decreasing the spot-to-spot distance to 642 µm allows up to 1176 spots to be printed on a single Lab-Tek slide, thereby accommodating samples from more than three 384-well plates.

Reverse transfection by manual spotting, for example, into 8-well Lab-Tek chambers is also possible. Usually, we perform this by placing a mask underneath the Lab-Tek chamber to facilitate a regular spot-to-spot spacing. Typical spot volumes are 0.2 µL, and about 9 spots can be printed into one of the 8-well chambers.

This all-in-one mixture thereby expedites sample preparation time and provides the reagents necessary for cell adherence on uncoated glass surfaces. In the second step, cells are plated onto these arrays in complete growth medium without further changes before data acquisition and analyses. In addition, we found that this transfection mixture is highly suited to a lower density of cells than previously used, ultimately allowing more detailed image analysis. Reducing in this way the reverse transfection protocol to two steps allows automation of the entire procedure as required for large-scale projects and is different from earlier protocols (6,7) that involved medium changes or the addition of serum. One problem when preparing arrays of siRNAs targeting endogenous genes is the subsequent location of the exact site of the spot-

ted material. To address this, we either used directly labeled siRNAs (Figures 1–3) or, to make such down-regulation cell arrays more universal and less expensive, unlabeled siRNAs were mixed with a nonrelevant Cy3-labeled DNA oligonucleotide serving as the transfection marker.

In the first phase, we compared HeLa, MCF7, COS7L, and HEK293 cells for their transfection efficiencies, growth behavior, and morphology. The highest transfection efficiencies (>95%) were achieved with HEK293 cells. However, these cells have the disadvantage that they tend to grow on top of each other, making automated image acquisition and analysis and, in particular, focus identification and cell segmentation, difficult. In addition, of all the cell types tested, they were the least adherent, and 24 h after plating cells onto spotted siRNAs, they had already detached. The lowest transfection efficiencies (70%) were achieved with COS7L cells. With MCF7 and HeLa cells, comparable transfection efficiencies of 80%–90% were obtained, and even 50 h after plating, HeLa cells were still highly adherent in the spot areas. For subsequent experiments, HeLa cells were used.

As a first test of our modified protocols in applications to down-regulate endogenous target genes, we designed a number of siRNA oligonucleotides against known proteins of the secretory pathway, including the β subunit of the coat protein complex COPI, an essential proteinaceous coat required for membrane transport through and the integrity of the Golgi complex (8). Cell arrays produced with these siRNAs were incubated for 44 h before fixing and staining with a monoclonal anti-β-COP antibody to monitor down-regulation of endogenous β-COP in individual cells. In the cell cluster where the β-COP-specific siRNA (siβ-COP_{161}) could be visualized in the rhodamine (marker) channel, almost no immunostaining of the β-COP protein in comparison to nontransfected cells outside the spot cluster could be observed, indicating effective down-regulation of the target protein by the labeled siRNA (Figure 1, A–C). In clusters where a rhodamine-labeled control siRNA known to have no target in mammalian cells was transfected, cells appeared to have normal β-COP staining, which was indistinguishable from those cells outside the spot area (Figure 1D). Quantification demonstrated that in β-COP-specific siRNA-transfected cells, only about 15% of β-COP-specific staining remained compared to control transfected cells (Figure 1E). When an identical but unlabeled siRNA against β-COP was co-transfected with the Cy3-labeled marker DNA oligonucleotide, endogenous β-COP was also efficiently suppressed (Figure 1E), suggesting that the addition of the labeled DNA oligonucleotide as a marker for the spot and transfected cells has only little effect on the uptake and efficacy of the target-specific siRNA molecules. We performed a control experiment in parallel, using "conventional" transfection of HeLa cells with the siβ-COP_{161} oligonucleotides to determine the extent of down-regulation as determined by Western blot analysis. As shown in Figure 1F, the levels of β-COP protein were reduced to similar levels as that observed by the analysis of the cell array, while tubulin was unaffected. Together, this indicates that, with respect to gene down-regulation, the cell array approach gives comparable results to biochemical techniques.

We also observed that within the global boundary of the spot, a number of the cells had no detectable rhodamine fluorescence, although the β-COP staining was clearly reduced. While measuring these cells, we observed that the average total intensities of the β-COP staining was in fact even lower than in those cells where the rhodamine-labeled siRNA molecules were still visible (Figure 1E). Because it was therefore clear that the down-regulation was also effective in all the cells within the global area of the spot, for subsequent evaluation we took all the cells within this area into account. One likely explanation of this visual disparity is that the rhodamine label of the siRNA is partially degraded during siRNA processing in the cell. To further test the quality of the quantitative analysis from such cell arrays, we designed a second siRNA against β-COP (siβ-COP_{1566}), which also caused a visible reduction in the level of β-COP protein; however, the quantification

confirmed that this was not as effective as the first oligonucleotide siβ-COP_{161} (Figure 1E). Therefore, such siRNA cell arrays also appear to be a useful means to compare the efficacy of multiple siRNA molecules (7). When siRNAs against Sec31, a component of the COPII complex (9) and against the Golgi matrix protein GM130 (10) were transfected, little effect on the strength of the β-COP staining was observed compared to control transfected cells, further highlighting the specificity of the approach (Figure 1E). The down-regulation of GM130 and Sec31 was however effective in these cells when checked by Western blot analysis (Figure 1F; data not shown).

We next applied the siRNA cell array to a functional assay in living cells. In particular, we were interested in screening for the effect of down-regulating individual components of the secretory pathway on the secretion of a specific transport marker. To perform this assay, we made use of recombinant adenoviruses encoding a fluorescently tagged temperature-sensitive variant of the viral glycoprotein VSV-G (ts-O45-G; References 4 and 11). This marker is particularly well suited to such assays because, at its restrictive temperature, it remains misfolded in the ER, but on lowering the temperature, it is rapidly transported to the cell surface. Visual analysis of the arrays revealed that in the spots containing siRNA against β-COP, the transport of the ts-O45-G to the cell surface was severely reduced in many of the cells (Figure 2A). In contrast, within the spot containing the control siRNA, the uptake did not apparently influence the transport (Figure 2B). For each spot, the transport efficiency was determined and thereby a measurement of the effectiveness of the siRNA in this functional assay. The control siRNA and DNA oligonucleotides alone had no significant effect on ts-O45-G secretion, whereas in the cells depleted of β-COP, transport was reduced to less than 40% of the control level. Furthermore, even in the spot containing the less effective siRNA against β-COP_{1566}, the

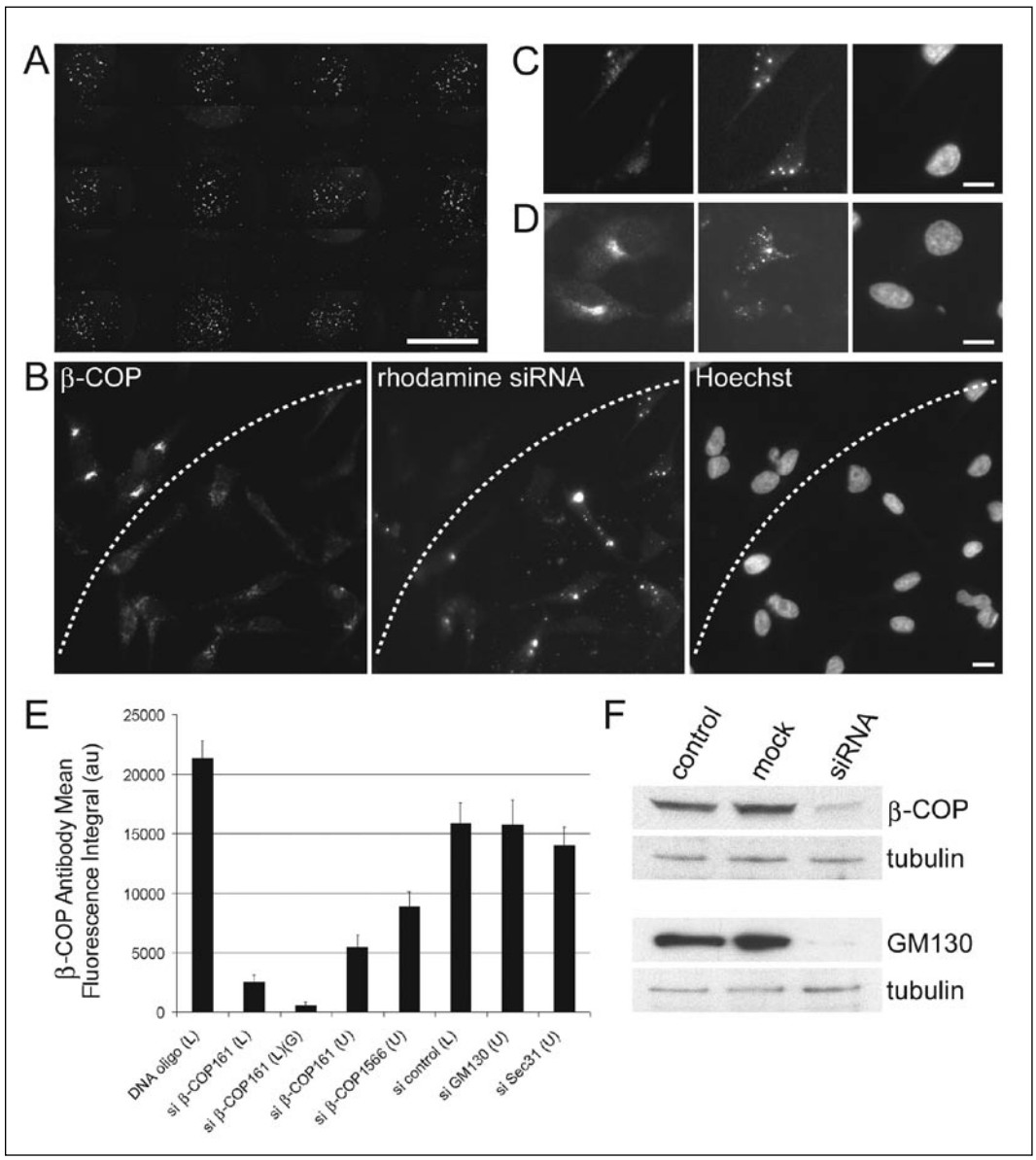

Figure 1. Specific down-regulation of endogenous β-COP on a small interfering RNA (siRNA) cell array in HeLa cells. (A) Example of a 4 × 3 array of rhodamine-labeled siRNA oligonucleotides against β-COP, and (B) their effect on the down-regulation of β-COP protein within the limit of the spotted area, as indicated by the dotted line. (C) Further enlargement of the cells within the area of this spot shows lack of β-COP staining in those cells containing the siRNA molecules, (D) whereas within the area of a rhodamine-labeled control (nonsilencing) siRNA spot, normal β-COP staining in those cells containing the siRNA molecules is observed. Bars indicate 500 µm in panel A and 10 µm in panels B–D. (E) A quantification of the β-COP immunostaining in spots containing siRNA oligonucleotides against various proteins of the secretory pathway. L denotes that the oligonucleotides were labeled, U denotes that they were unlabeled but co-transfected with the Cy3 marker DNA oligonucleotide, and G denotes that the measurement was made from the global area of the spot. (F) The efficacy of the siRNAs against β-COP and GM130 was also confirmed by Western blot analysis. Blots for tubulin from the same cells are shown to indicate protein loadings. Oligo, oligonucleotide; si, small interfering; au, arbitrary units.

transport efficiency was also reduced. These data are in good agreement with the role of COPI in retrograde transport from post-ER membranes (13, and references therein), and a reduction of cellular β-COP levels down to 15% of control values should clearly affect ts-O45-G transport as observed here. However, as β-COP is only indirectly involved in anterograde transport, the amounts of β-COP in siRNA-treated cells may still be enough to allow some ts-O45-G to be transported and provides a possible explanation for still 40% of ts-O45-G arriving at the plasma membrane in our experiments at strongly reduced β-COP levels.

Of particular interest, however, was that in the spots of siRNA against GM130 and Sec31, ts-O45-G transport was reduced to approximately 50% of control values (Figure 2C). Although these results are perhaps not surprising because these proteins are important components of the secretory pathway, they provide evidence that such siRNA cell arrays are sufficiently sensitive to be used in functional assays such as this one to screen large panels of siRNA molecules designed against endogenous targets.

Finally, we tested our reverse transfection protocol for its ability to be able to deliver both DNA and siRNA molecules into the same cells. Such a possibility is important for large-scale screening projects in which the cDNA encoding a protein of unknown function is available, but an antibody is not. In such a case, it is imperative to know that an siRNA targeted against the protein of unknown function is effectively down-regulating the protein. To demonstrate this, we created an array with spots containing both a cDNA encoding CFP-β-COP and the corresponding siRNA (Figure 3). Between 20 and 40 CFP-β-COP-expressing cells were clearly visible in those spots transfecting either the cDNA alone (Figure 3A) or the cDNA with the control siRNA oligonucleotides (Figure 3C). In contrast, the expression of CFP-β-COP was almost not detectable when the siβ-COP_{161} oligonucleotides were co-transfected with the CFP-β-COP cDNA (Figure 3B).

Such an siRNA array should prove an ideal means to utilize the already available large resources of fluorescently tagged cDNAs of unknown function (see http://gfp-cdna.embl.de/; Reference 12) in combination with libraries of siRNA molecules, and thereby determine siRNA efficacy prior to their routine use. Together, our

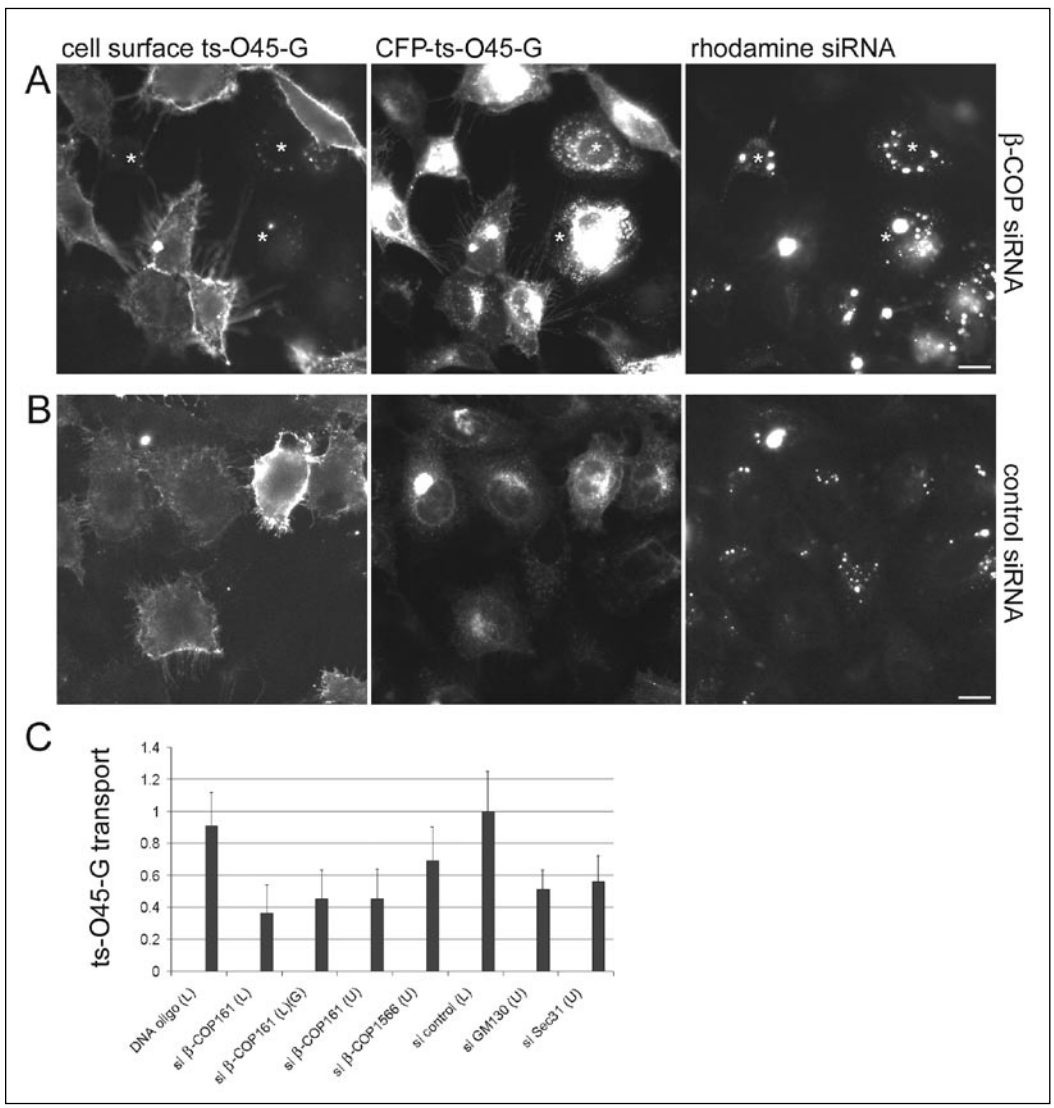

Figure 2. Use of a small interfering RNA (siRNA) cell array in an assay to measure ts-O45-G transport to the plasma membrane in HeLa cells. (A) Images from within a spot of transfected siRNA against β-COP showing the presence of the secretory marker ts-O45-G on the cell surface, the total CFP-ts-O45-G in the cells, and the presence of the labeled siRNAs. Asterisks mark those cells showing the presence of siRNAs, but no transport of ts-O45-G to the cell surface. (B) Similar experiment as shown in panel A but using a control siRNA. Bars indicate 10 µm. (C) Quantification of ts-O45-G transport to the cell surface in spots containing siRNA oligonucleotides against various proteins of the secretory pathway. L denotes that the oligonucleotides were labeled, U denotes they were unlabeled but co-transfected with the Cy3 marker DNA oligonucleotide, and G denotes that the measurement was made from the global area of the spot. Oligo, oligonucleotide; CFP, cyan fluorescent protein; si, small interfering.

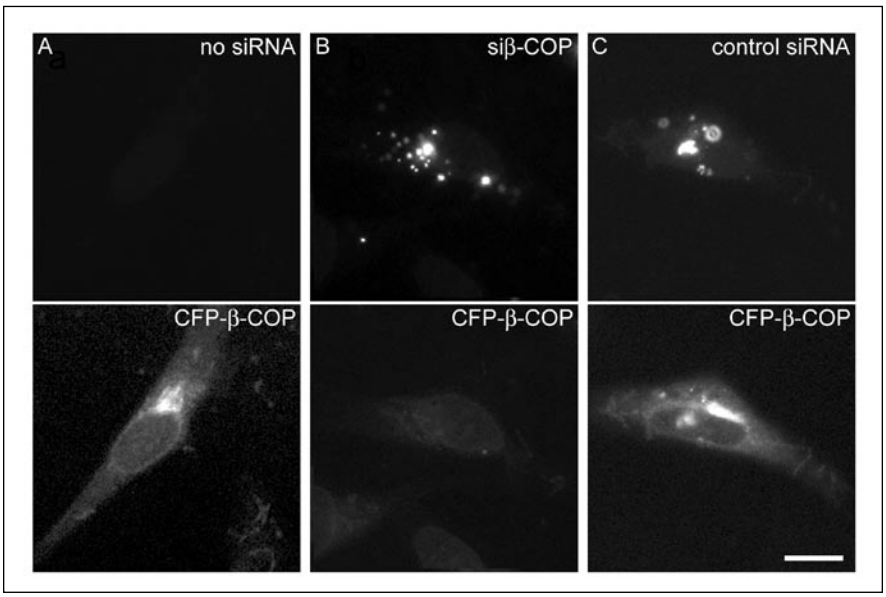

Figure 3. Co-transfection on arrays spotted with cDNA and small interfering RNA (siRNA) molecules in HeLa cells. (A) Example of a CFP-β-COP-expressing cell in a spot transfected with the respective plasmid expression vector only. (B) Cell showing co-transfection of CFP-β-COP and a corresponding siRNA, resulting in the lack of cDNA expression. No cells expressing CFP-β-COP could be detected in these spots. (C) Cell showing co-transfection of CFP-β-COP and a control siRNA. Bar indicates 10 µm. CFP, cyan fluorescent protein.

results show that the improved protocols we have developed for the creation of cell arrays are highly robust, equally applicable to cDNA overexpression and siRNA down-regulation, and are suitable for application in high-resolution functional assays in living cells to determine protein function.

ACKNOWLEDGMENTS

We thank Brigitte Joggerst for technical assistance. This work has been supported by the BMBF with grants 01GR0101 and 01KW0013 and by a grant from the Verbundforschung Baden-Wuerttemberg (grant no. 24-720.431-1-2/2) to R.P.

COMPETING INTERESTS STATEMENT

The authors declare that they have no competing interests.

REFERENCES

1. **Ziauddin, J., and D.M. Sabatini.** 2001. Microarrays of cells expressing defined cDNAs. Nature *411*:107-110.
2. **Elbashir, S.M., J. Harborth, W. Lendeckel, A. Yalcin, K. Weber, and T. Tuschl.** 2001. Duplexes of 21-nucleotide RNAs mediate RNA interference in cultured mammalian cells. Nature *411*:494-498.
3. **Gonczy, P., C. Echeverri, K. Oegema, A. Coulson, S.J. Jones, R.R. Copley, J. Duperon, J. Oegema, et al.** 2000. Functional genomic analysis of cell division in C. elegans using RNAi of genes on chromosome III. Nature *408*:331-336.
4. **Pepperkok, R., J. Scheel, H. Horstmann, H.P. Hauri, G. Griffiths, and T.E. Kreis.** 1993. Beta-COP is essential for biosynthetic membrane transport from the endoplasmic reticulum to the Golgi complex in vivo. Cell *74*:71-82.
5. **Keller, P., D. Toomre, E. Diaz, J. White, and K. Simons.** 2001. Multicolour imaging of post-Golgi sorting and trafficking in live cells. Nat. Cell Biol. 3:140-149.
6. **Mousses, S., N.J. Caplen, R. Cornelison, D. Weaver, M. Basik, S. Hautaniemi, A.G. Elkahloun, R.A. Lotufo, et al.** 2003. RNAi microarray analysis in cultured mammalian cells. Genome Res. *13*:2341-2347.
7. **Kumar, R., D.S. Conklin, and V. Mittal.** 2003. High-throughput selection of effective RNAi probes for gene silencing. Genome Res. *13*:2333-2340.
8. **Guo, Q., E. Vasile, and M. Krieger.** 1994. Disruptions in Golgi structure and membrane traffic in a conditional lethal mammalian cell mutant are corrected by epsilon-COP. J. Cell Biol. *125*:1213-1224.
9. **Salama, N.R., J.S. Chuang, and R.W. Schekman.** 1997. Sec31 encodes an essential component of the COPII coat required for transport vesicle budding from the endoplasmic reticulum. Mol. Biol. Cell *8*:205-217.
10. **Nakamura, N., C. Rabouille, R. Watson, T. Nilsson, N. Hui, P. Slusarewicz, T.E. Kreis, and G. Warren.** 1995. Characterization of a cis-Golgi matrix protein, GM130. J. Cell Biol. *131*:1715-1726.
11. **Liebel, U., V. Starkuviene, H. Erfle, J.C. Simpson, A. Poustka, S. Wiemann, and R. Pepperkok.** 2003. A microscope-based screening platform for large scale functional analysis in intact cells. FEBS Lett. *554*:394-398.
12. **Simpson, J.C., R. Wellenreuther, A. Poustka, R. Pepperkok, and S. Wiemann.** 2000. Systematic subcellular localization of novel proteins identified by large-scale cDNA sequencing. EMBO Rep. *1*:287-292.
13. **Stephens, D.J., and R. Pepperkok.** 2002. Illuminating the secretory pathway. When do we need vesicles? J. Cell Sci. *114*:1053-1059.

Received 26 April 2004; accepted 9 June 2004.

Address correspondence to Rainer Pepperkok, European Molecular Biology Laboratory (EMBL), Meyerhofstrasse 1, 69117 Heidelberg, Germany. e-mail: pepperko@embl-heidelberg.de